AGU PUBLICATIONS

[Geophysical Research Letters]

Supporting Information for

Proglacial lakes control glacier geometry and behavior during recession

Jenna L. Sutherland[1], Jonathan L. Carrivick[1], Niall Gandy[2], James Shulmeister[3], Duncan J. Quincey[1], Stephen L. Cornford[4]

[1, 2]University of Leeds, [3]University of Canterbury, [4]University of Swansea

Contents of this file

- Text S1 to S4
- Figures S1 to S6
- Tables S1 to S3

Additional Supporting Information (Files uploaded separately)

Captions for Movies S1 to S3

Introduction

This supporting information comprises additional details of the datasets used in this study and their analysis. Text S1 provides additional information on the model initial conditions, including LGM bed topography and model parameters, supported by Figure S1 and Table S1. Text S2 outlines the procedure and results (Figure S2) for the model spin up. Text S3 discusses the experimental design of the model simulations, supported by Table S3, including how the idealised climate was prescribed and how the LAKE simulation was initiated. An extended description of the sensitivity analysis is given in Text S4 and Table S2, the results of which are given in Figure S3. Figures S4-S6 are included to provide additional illustration to the results. Movie S1 and S2 are the full retreat simulations for LAND and LAKE respectively. Movie S3 presents the LAKE simulation where ice thickness has been inverted to clearly show the effect of the lake on the ice front.

Text S1. Model initial conditions

S1.1 Bed topography

Before beginning the numerical modelling, we needed to consider the Last Glacial Maximum (LGM) bed conditions. We cannot assume that contemporary topography is an appropriate representation of the glacier bed beneath the Pukaki Glacier. The Pukaki Glacier occupied an area where Lake Pukaki now exists, for which standard digital elevation models (DEMs) represent the water surface and not the underlying bathymetry, thus obscuring the former glacier bed topography. To produce a DEM more representative of LGM conditions, the water depth of Lake Pukaki (Irwin, 1970) was subtracted from the modern DEM. The lake is only 98 m deep at its deepest, which is relatively shallow when compared to many other lakes in New Zealand that have beds below sea level (e.g. Lake Wakatipu, >300 m deep; Sutherland *et al*., 2019).

Geophysical data from Lake Ohau, in an adjacent valley to Lake Pukaki, indicate that the lake basin there contains up to 140 m of sediment deposited directly on top of bedrock (Levy *et al*., 2018). Sediment cores collected from Lake Ohau reveal that these sediments have accumulated since lake formation at the end of the LGM ~ 17 ka (Levy *et al*., 2018). Seismic surveys subparallel to the Pukaki basin provide estimates of the subsurface locations of bedrock also presently covered by thick layers of sediment (Kleffman *et al*., 1998; Long *et al*., 2003). Based on these studies, we contend that substantial sediment deposition has occurred in the Pukaki valley since the LGM and it is likely that the Pukaki Glacier bed is buried by Late Glacial and post-glacial sediments. Indeed, McKinnon *et al*. (2012) estimated post-LGM sediment thickness distribution (and area extent) within the Pukaki valley, revealing up to 384 m of post-LGM infill. Therefore, in this study, we used these estimates of bedrock elevation as a constraint on the modelled bed profile for the LGM. These bed elevation data were subsequently merged with the modern DEM to produce a surface that we suppose is more representative of LGM bed conditions (**Figure S1**) than simply using a modern DEM. It is highly unusual to know the bathymetry of a proglacial lake, especially one formed from the LGM, and this knowledge (in addition to the cosmogenic nuclide dating of the moraines that encircle Lake Pukaki) is further justification for our choice of site for this study.

S1.2 Model domain and parameters

We set up our model domain to cover 64 km by 128 km. For computational efficiency during the spin up simulation (**Text S2**) we set a 500 m x 500 m grid refined three times around the grounding line of Pukaki to produce a maximum horizontal resolution of 125 m (**Figure S2**). For the LAKE and LAND simulations we used a 250 m by 250 m horizontal grid resolution across the entire model domain. The simulations have 10 vertical levels. Ice surface temperature was held constant at an isothermal value of 268 K in all simulations (**Table S1**).

Text S2. Model spin up

Numerical modelling results can be heavily influenced by the starting condition. In this case it was imperative that the starting condition of ice thickness was that of a glacier in equilibrium, to be sure that subsequent glacier changes were only a product of a modelled forcing. In this study, ice extent in the spin up model run was controlled by the surface mass balance (SMB). We imposed the initial SMB by the following equation, where the Equilibrium Line Altitude (ELA) prescribed was 1465 m;

$$SMB = (surface\ elevation - ELA) * 0.0025$$

This allowed the Pukaki Glacier to advance to its LGM position (Figure S2), comparable to empirical reconstructions (e.g. Barrell *et al.*, 2011), and other modelled ice thicknesses of the Pukaki Glacier (e.g. Golledge *et al.*, 2012; James *et al.*, 2019). The ice thickness at the end of this spin up simulation was used as the initial condition for LAND and LAKE simulations which began at a stable ice volume with ice grounded on the topography ~ 2 km down-valley from the lip of its over-deepened basin.

Text S3. Model Experimental design

S3.1 Parameterisation of climate

The motivation for this study was to assess the impact of a proglacial lake on ice dynamics, not to produce more realistic glacier changes or an absolute chronology of events. Based on an accumulation area ratio (AAR) analysis of reconstructed glaciers at the LGM, Porter (1975) estimated that the LGM ELA was 1225 m and that the Late Glacial ELA inside the Birch Hill moraine limit was 500 ± 50 m lower than the modern day (2100 m; Chinn *et al.*, 2012). The ELA for the Birch Hill re-advance is therefore taken to be 1600 m. The way in which we prescribed a steadily warming climate is given as follows;

$$ELA = 1465 + (10000 * 0.05)$$

where 1465 is the initial starting condition, 10,000 is the length of the model run, and 0.05 represents the rate of ELA rise.

S3.2 Initiating the 'LAKE' simulation

Given that the present-day surface of Lake Pukaki lies at an elevation of 525 m a.s.l. we reset the elevations relative to the lake level. we lowered the topography of the whole model domain by 525 m to effectively bring the lake surface down to sea level (0 m a.s.l) in order to initiate the LAKE simulation. This method enabled us to then prescribe calving and subaqueous melt fluxes since BISICLES can only simulate such processes when the glacier margin is at zero elevation. The ELA in the LAKE simulation was also lowered by 525 m to account for the topographic lowering. Therefore, we take the ELA (initial starting condition) in the LAKE simulations to be 925 m.

Our choice of ice sheet model was based on accounting for grounding line dynamics induced by proglacial lakes and the issue in how we applied the model to simulate an inland lake is not a concern for the process-representation. Lacustrine termini are thought to experience fewer perturbations (e.g. tidal flexure, high subaqueous melt rates) and are therefore inherently more stable than tidewater termini. Water circulation in a proglacial water body determines when and how heat reaches glacial ice and affects melting. In marine-terminating environments, relatively warm ocean water can be drawn towards an ice margin by water circulation patterns caused by the relative buoyancy of that freshwater within the saline water. Water circulation in marine settings can be driven by density differences (Farmer and Freeland, 1983; Motyka et al., 2003), tides (Mortensen et al., 2011) or winds (Straneo et al., 2010), but since the water of a proglacial lake is fresh, such a circulation will not arise. All heating and cooling processes in a lake are therefore local and take place in a closed system, as opposed to marine environments where heat can be transported long distance from the ocean, which effectively acts as an infinite reservoir of heat (Truffer and Motyka, 2016).

Near-terminus surface slopes of tidewater glaciers are typically steeper than lake-calving termini, resulting in near-terminus ice speeds differing by an order of magnitude. Retreating tidewater glaciers often flow at speeds of 5-10 km a^{-1}, compared to 100-1000 m a^{-1} for lake-terminating glaciers (Truffer and Motyka, 2016). Grounded tidewater termini are typically highly crevassed and characterized by steep topography, fast flow, high strain rates and frequent calving activity. In contrast, many lake-calving glaciers form floating tongues that are characterized by lower surface gradients, flatter topography, slower flow, lower strain rates, less crevassing, and infrequent but massive calving activity, often in the form of large tabular blocks. Such is the case for lacustrine terminating glaciers in Alaska, New Zealand and Chilean Patagonia. However, this distinction does not hold universally, departures from this model are the large east Patagonian lakes, where they are exposed to relatively intense solar heating, and lake water temperatures can exceed 4 ºC in summer (Truffer and Motyka, 2016). Subglacial discharge could be buoyant in such water, although density difference is significantly smaller than that between fresh and saline waters. The onset of circulation, together with the thermal forcing from entrained warm water, would lead to moderate rates of subaqueous melting that are below those observed at temperate tidewater glaciers, but significantly above those observed at smaller lakes. The largest of these lakes, Lago Argentino, lying at the terminus of Glaciar Upsala, has a maximum water depth at the grounding line of ~500 m, deep enough to allow part of the glacier tongue to float. Lago Argentino could serve as an analogue for Lake Pukaki in terms of energy balance, temperature and water circulations. However, the surface area of Lago Argentino is ~1400 km^2, an order of magnitude higher than that of Lake Pukaki (~180 km^2). It is also noteworthy that glaciers that exit into the east Patagonia lakes (e.g. Upsala, Perito Moreno, and Viedma) are generally not afloat and do not calve tabular icebergs, while those in Alaska and Chilean Patagonia do. Generally, the east Patagonian lake-calving glaciers appear to have more in common with tidewater glaciers in terms of glacier speeds and terminus morphology (Venteris, 1999; Stuefer et al., 2007; Sakakibara and Sugiyama, 2014).

Text S4. Sensitivity analysis

A calving rate and a subaqueous melt rate needed to be calculated and prescribed in the LAKE simulations. Calving and subaqueous melt research is disproportionately focused towards tidewater glacier margins (Van der Veen, 2002; Benn et al., 2007). A sparsity of quantitative data means that these processes and their associated drivers at lacustrine ice-margins remain poorly understood (Purdie et al., 2016). Therefore, constraining rates based on present-day observations of exiting proglacial lakes is difficult. **Table S2** shows highly variable calving and melt rates in proglacial lakes depending on many factors such as location and water depth.

Based on the differences and assumptions described above, we aimed to test the sensitivity of the model to (i) different types of calving model, (ii) the calving rate and (iii) the subaqueous melt rate (**Table S3**). The sensitivity simulations were run at a horizontal model resolution of 500 m for 4,000 years (from 18 ka to 14 ka). This enabled enough time to force the terminus into the lake and well back through the over-deepening in order to assess changes in model output.

S4.1 Calving rate

Existing data from modern glaciers consistently show that calving occurs much more slowly in lakes than in comparable tidewater settings. Lacustrine calving rates are typically an order of magnitude lower than that of tidewater termini (Funk and Rothlisberger, 1989; Warren et al., 1995; Warren and Aniya, 1999; Benn et al., 2007; Truffer and Motyka, 2016). Such differences have been attributed to contrasts in water densities, upwelling rates (and associated turbulent heat transfer), subaqueous melt rates, frontal oversteepening and longitudinal strain rates (Funk and Röthlisberger, 1989; Warren et al., 1995; Van der Veen, 2002). Warren and Kirkbride (2003) confirm that calving correlates linearly with water depth in freshwater.

There is a strong contrast in calving mechanisms and rates between tidewater and freshwater settings (Warren and Kirkbride, 2003). Thermal undercutting and buoyancy-driven ice calving are the primary controls of retreat in most lakes. Thermo-erosional notches in the calving front of glaciers that terminate in lakes may be formed when rates of melting at the waterline are higher than subaerial or subaqueous rates of melting. They have been observed at a variety of lake-calving glaciers in New Zealand (Warren and Kirkbride, 2003; Röhl, 2006; Dykes et al., 2010), Alaska (Trussel et al., 2013), Patagonia (Truffer and Motyka, 2016), and east Greenland (Mallalieu et al., 2020).

S4.2 Subaqueous melt rate

Many lacustrine subaqueous melt rates reported in the literature are conceptual or have been reported from supraglacial lakes and ice cliffs, albeit a similar process but on a much smaller scale. Several different methods have been applied to model subaqueous melt rates and as such, their measured units vary from mm hr^{-1} to m a^{-1}. Some report a calving flux (e.g. m^3) whilst others report a calving rate (e.g. m a^{-1}). Subaqueous melting is the least well-constrained term, however, could account for significant portions of total ice retreat. The formulas for subaqueous melt rates in numerical models, that are mainly derived from experiments and match inferred rates from studies of Antarctic icebergs, apply to clean ice. The submerged faces of a glacier terminating in a lake are likely to be covered to varying degrees with sediments. Besides other minor factors melt rates have been shown to decrease with increasing water pressure at depth. The influence of water pressure is significant for melting processes in ice-contact lakes as water depths often exceed 100 m.

S4.3 Results of sensitivity analysis

Our sensitivity testing (**Figure S3**) revealed that varying the subaqueous melt rate produced morphological differences, such as the existence or absence of floating ice tongues. Subaqueous melting had a negligible effect on grounding line position in our model but had a significant effect on terminus position.

Where the combination of ice thicknesses and water depth satisfies the flotation criterion within the model, an ice shelf is formed. Low subaqueous melt rates (e.g. 0 - 10 m a^{-1}) result in a configuration where a large ice shelf was permitted to form during retreat with only a narrow band of exposed water. In contrast, when high or extreme subaqueous melting was prescribed (e.g. 100 m a^{-1}), the resulting configuration forced the removal of the ice shelf with little or no floating ice during retreat and a relatively large area of exposed water. The subaqueous melt rate therefore determines how much floating ice is present. Subaqueous melt drives retreat of terminus position, however, if the floating ice has a slightly larger extent, the impact on grounded ice extent, volume and velocity is still negligible. Changing the calving rate was also found to have a negligible effect on the overall pattern of retreat (**Figure S3**). This is because the ice terminus was wedge-shaped (when a melt rate >10 m a^{-1} was prescribed) and so the calving rate had little impact. Calving at the ice front plays only a minor role and our experiments are weakly sensitive to its representation in the model. Calving has much less control on grounding line retreat. As a result, a distinct calving model for lakes will not have any impact in our experiments. We acknowledge that this might not necessarily always be the case for different time intervals or settings (e.g. a colder climate). Most importantly, we show that both changing the calving or subaqueous melt rates have a negligible impact on grounding line position.

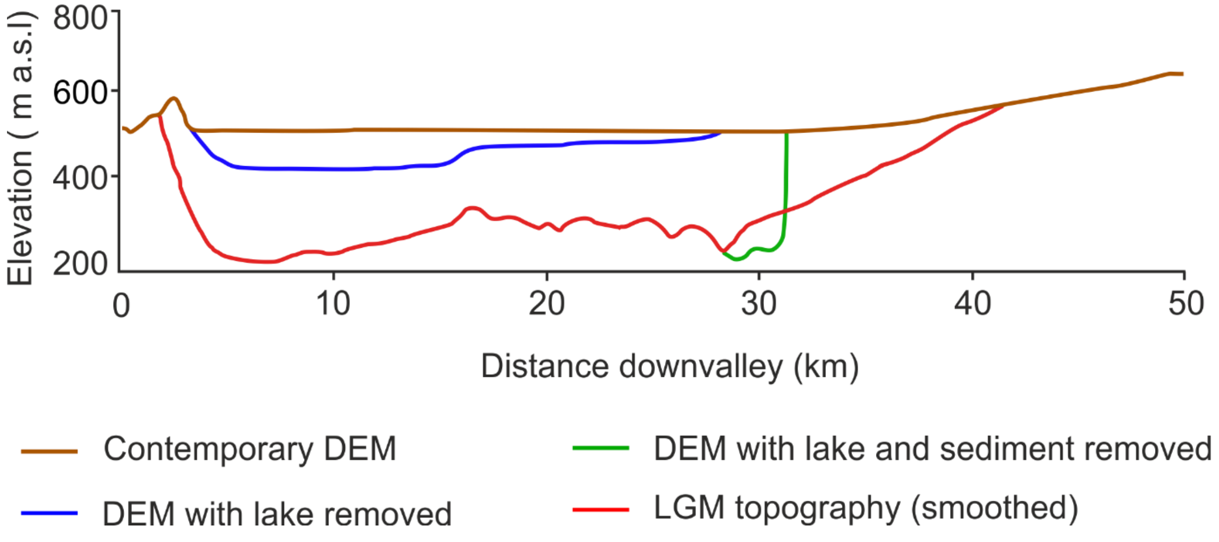

Figure S1. LGM bed profile. Profile taken along X-Y transect in **Figure 3a**

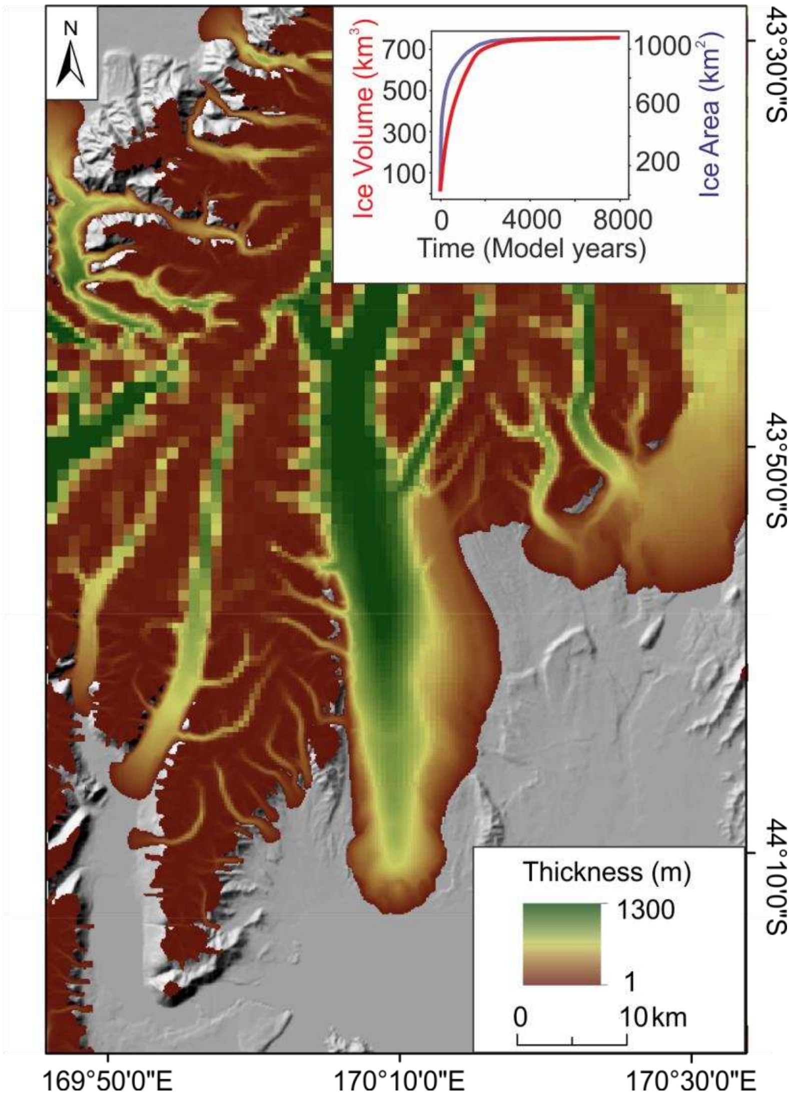

Figure S2. Initial ice thickness and extent from the equilibrium spin up LGM ice simulation at 18 ka (a description of which is given in **Text S2**). Inset shows the evolution of ice volume and area during the spin-up simulation. Horizontal model resolution at the ice margin s 125 m with 3 levels of refinement.

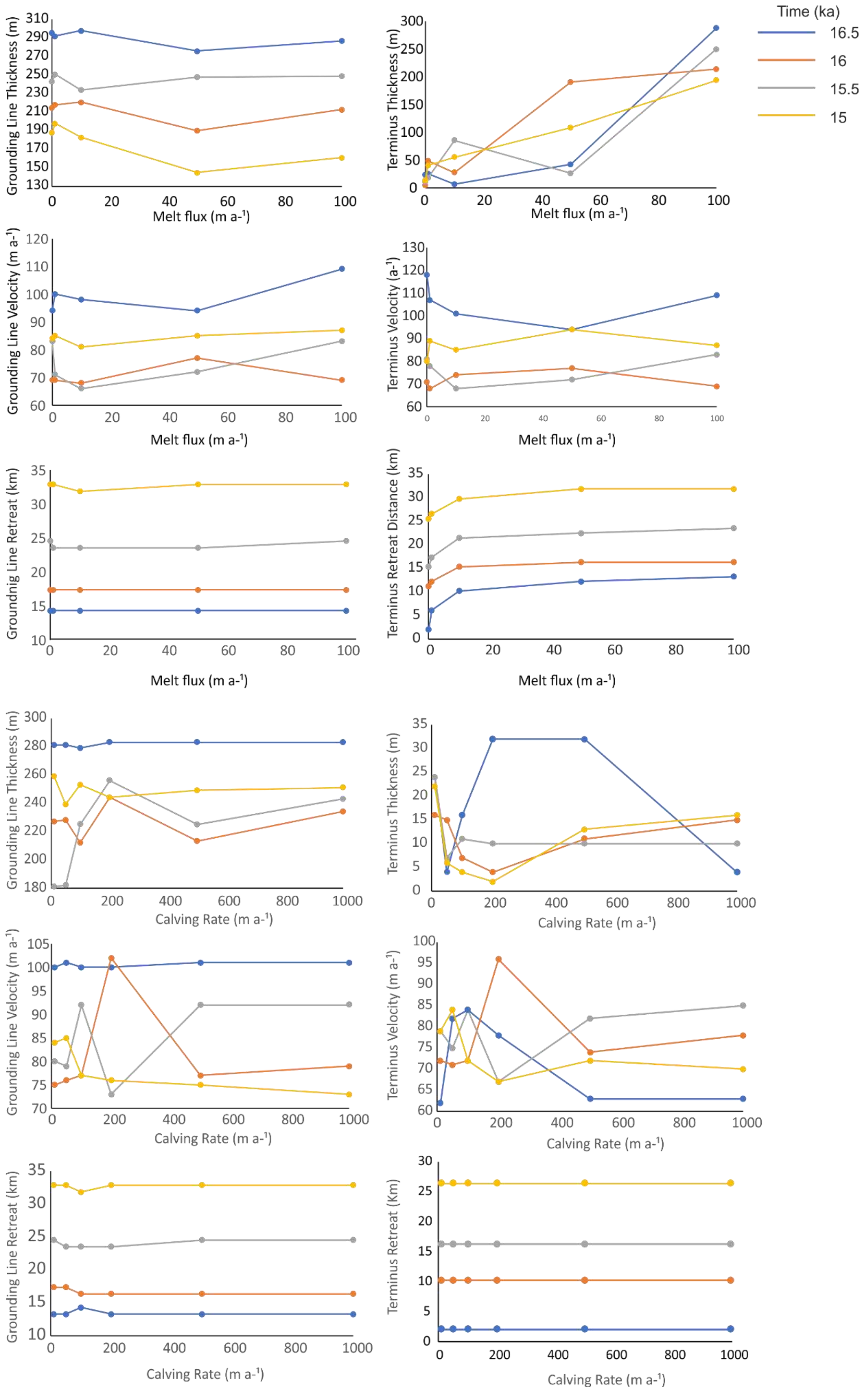

Figure S3. Effects of changing subaqueous melt and calving rate on grounding line and terminus position, ice thickness, and velocity. Parameters and values reported in **Table S3**

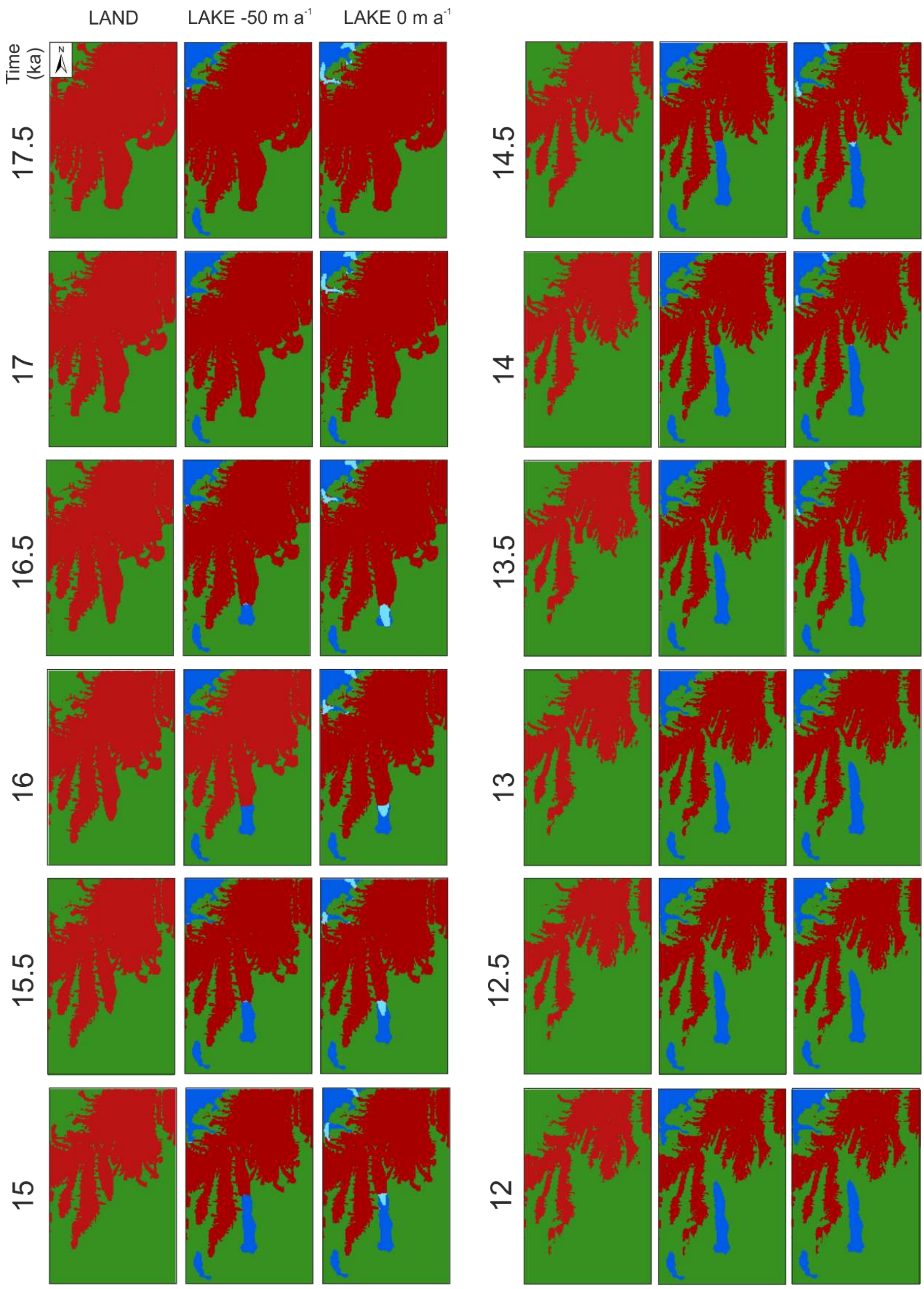

Figure S4. Model domain gridded into areas of open land (green), open water (dark blue), Grounded ice (red), and floating ice (light blue) for LAND and LAKE with -50 m a-1 subaqueous melt rate prescribed, and LAKE with 0 m a-1 subaqueous melt rate prescribed. Plotted every 500 years from 17.5 ka to 12 ka. Note difference in terminus position and extent of floating ice between both LAKE simulations, however, grounding line position remains the same.

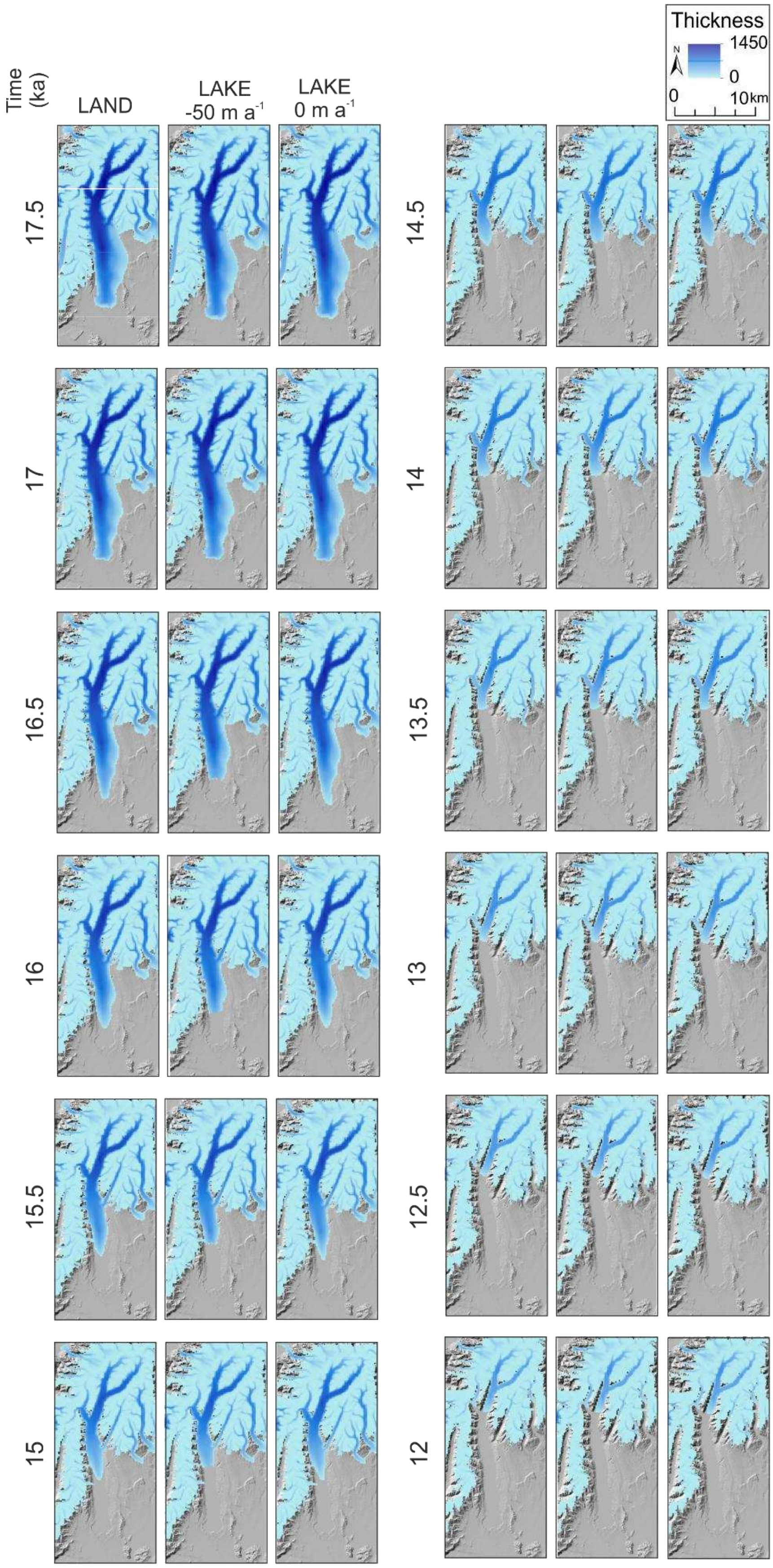

Figure S5. Ice thickness maps for LAND and LAKE with -50 m a-1 subaqueous melt rate prescribed, and LAKE with 0 m a-1 subaqueous melt rate prescribed. Plotted every 500 years from 17.5 ka to 12 ka. Note difference in terminus position between both LAKE simulations but grounding line thickness remains the same.

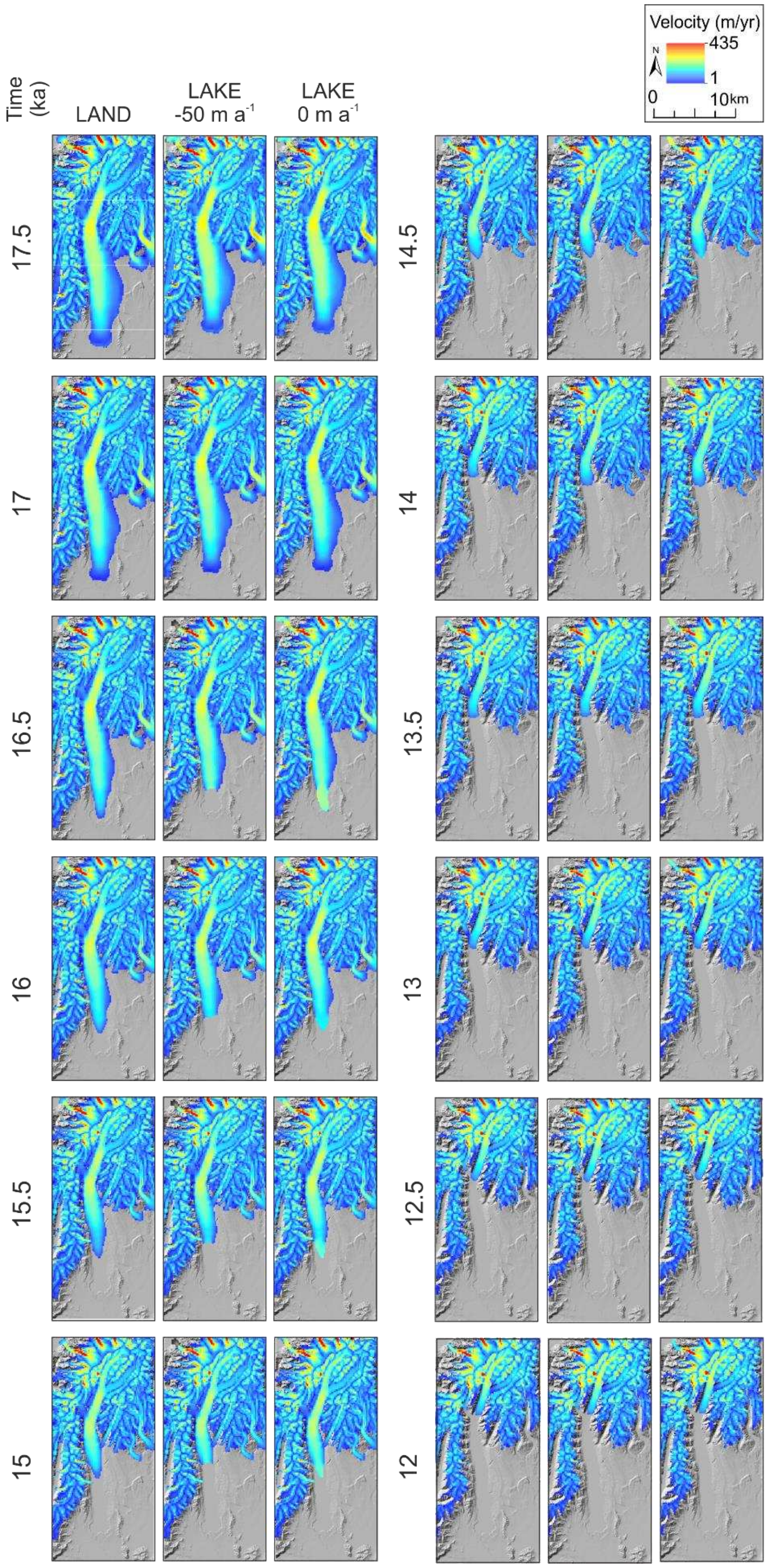

Figure S6. Ice velocity maps for LAND and LAKE with -50 m a-1 subaqueous melt rate prescribed, and LAKE with 0 m a-1 subaqueous melt rate prescribed. Plotted every 500 years from 17.5 ka to 12 ka. Note difference in terminus position between both LAKE simulations, but ice velocity over the grounding line remains the same

Parameter	**Value**	**Units**
Sliding exponent	1	
Isothermal ice temperature	268	K
Ice density	918	Kg m^{-3}
Water density (freshwater)	1000	kg/m^{-3}
Domain length	128	Km
Domain width	64	Km
Maximum refinement	0.25	Km

Table S1. Key model parameters

Location	Glacier name	Calving Rate (m a^{-1})	Subaqueous melt rate (m a^{-1})	Reference	Explanatory notes
New Zealand	Maud	88	18	Warren and Kirkbride (2003)	Width and annually averaged measurements taken in Autumn 1994-95 Temperate Grounded Debris-covered Largely un-crevassed Calving face typically 20-40 m Grounded in shallow water (<20 m)
	Grey	47	18		
	Godley	47	18		
	Hooker	14	18		
	Ruth	18	18		
	Tasman	28	18		
		34		Röhl (2006)	Measurements taken between 2001 and 2003 Maximum water depth and average water depth along ice cliff of 180 m and 50 m respectively
			17.7	Kirkbride (1995)	
			40	Roehl (2002)	Average taken from different water temperatures
			25 ± 5	Hochstein et al. (1998)	Measured change in perimeter of a large, tabular iceberg which grounded in front of the ice cliff over 3 years
Argentina	Ameghino	275		Warren et al. (1995)	
	Moreno	800		Warren et al. (1995)	
Chile	Leon	880		Haresign and Warren (2005)	Temperate, grounded outlet of the North Patagonian Icefield. Mean water depth of 65 m Measurements taken between 2001 and 2002 Ice-proximal surface water temperatures of 6–7°C Waterline melt notches grow at rates of *c.* 0.8 m/day Unusually high calving rate
Alaska	Mendenhall	187		Motyka et al. (2003)	
British Columbia	Bridge	70		Chernos et al. (2016)	Study period 1983-2013 estimated calving flux of 0.0362 km^3
Himalaya	Lirung		4-14 m a^{-1}	Sakai et al. (1998)	Average observed supra-aqueous ice cliff melt during the melt season
	Ngozumpa		2.1 **cm hr^{-1}**	Benn et al. (2001)	Waterline notch measurement taken in 1998
Norway	Svartisheibreen	5		Kennett et al. (1997)	

Table S2. Calving and subaqueous melt fluxes from different settings. Note change in units for Ngozumpa Glacier (Benn et al., 2001) in cm hr-1

Experiment Name	Initial thickness	ELA (m a.s.l)	Subaqueous melt rate (m a^{-1})	Calving model	Calving rate (m a^{-1})
SPIN UP	James et al. (2019)	1465	N/A	N/A	N/A
SENSITIVITY_CALVING_FLUX	SPIN UP	0.05	0	Crevasse	**10**
	SPIN UP	0.05	0	Crevasse	**50**
	SPIN UP	0.05	0	Crevasse	**100**
	SPIN UP	0.05	0	Crevasse	**200**
	SPIN UP	0.05	0	Crevasse	**500**
	SPIN UP	0.05	0	Crevasse	**1000**
SENSITIVITY_CALVING_MODEL	SPIN UP	0.05	0	**Flotation**	100
	SPIN UP	0.05	0	**Rate proportional to speed**	100
	SPIN UP	0.05	0	**Crevasse**	100
	SPIN UP	0.05	0	**No Calving**	100
	SPIN UP	0.05	0	**Cliff Collapse**	100
	SPIN UP	0.05	0	**Damage**	100
	SPIN UP	0.05	0	**Maximum Extent**	100
			0	Crevasse	0
SENSITIVITY_MELT_FLUX	SPIN UP	0.05	**-1**	Crevasse	0
	SPIN UP	0.05	**-10**	Crevasse	0
	SPIN UP	0.05	**-50**	Crevasse	0
	SPIN UP	0.05	**-100**	Crevasse	0
LAND	SPIN UP	0.05	N/A	N/A	N/A
LAKE	SPIN UP	940	-50	Crevasse	100

Table S3. Summary of experimental set-up, sensitivity analysis and forcing

Movie S1. LAND simulation

Movie S2 LAKE simulation using the Crevasse Calving Model where the crevasse depth was set such that it removed ice shelves and floating ice thinner than 100 m. The calving flux and subaqueous melt flux were set to 100 m a^{-1} and -50 m a^{-1} respectively

Movie S3. LAKE simulation using the Crevasse Calving Model where the crevasse depth was set such that it removed ice shelves and floating ice thinner than 100 m. The calving flux and subaqueous melt flux were set to 100 m a^{-1} and -50 m a^{-1} respectively. Thickness has been inverted to clearly show the effect of the lake on the ice front

REFERENCES

Barrell, D. J. A., Andersen, B. G., Denton, G. H., and Smith-Lyttle, B. 2011. Glacial Geomorphology of the Central South Island, New Zealand, vol.27 GNS Science monograph (2011)

Benn, D. I., Warren, C. R., & Mottram, R. H. 2007. Calving processes and the dynamics of calving glaciers. *Earth-Science Reviews*, *82*(3-4), 143-179

Carrivick, J. L., and Tweed, F. S. 2013. Proglacial lakes: character, behaviour and geological importance. *Quaternary Science Reviews*, *78*, 34-52

Chernos, M., Koppes, M., and Moore, R. D. 2016. Ablation from calving and surface melt at lake-terminating Bridge Glacier, British Columbia, 1984-2013. *Cryosphere*, *10*(1)

Chinn, T., Fitzharris, B. B., Willsman, A., and Salinger, M. J. 2012. Annual ice volume changes 1976–2008 for the New Zealand Southern Alps. *Global and Planetary Change*, *92*, 105-118

Drost, F., Renwick, J., Bhaskaran, B., Oliver, H., and McGregor, J. 2007. A simulation of New Zealand's climate during the Last Glacial Maximum. *Quaternary Science Reviews*, *26*(19-21), 2505-2525

Dykes, R. C., Brook, M. S., and Winkler, S. 2010. The contemporary retreat of Tasman Glacier, Southern Alps, New Zealand, and the evolution of Tasman proglacial lake since AD 2000. *Erdkunde*, 141-154

Farmer, D. M., and Freeland, H. J. 1983. The physical oceanography of fjords. *Progress in oceanography*, *12*(2), 147-219

Funk, M., and Röthlisberger, H. 1989. Forecasting the effects of a planned reservoir which will partially flood the tongue of Unteraargletscher in Switzerland. *Annals of Glaciology*, *13*, 76-81

Gandy, N., Gregoire, L. J., Ely, J., Clark, C., Hodgson, D. M., Lee, V., Bradwell, T., and Ivanovic, R. F. 2018. Marine ice sheet instability and ice shelf buttressing of the Minch Ice Stream, northwest Scotland. *The Cryosphere*, *12*, 3635-3651

Golledge, N. R., Mackintosh, A. N., Anderson, B. M., Buckley, K. M., Doughty, A. M., Barrell, D. J., Denton, G. H., Vandergoes, M. J., Andersen, B. G., and Schaefer, J. M. 2012. Last Glacial Maximum climate in New Zealand inferred from a modelled Southern Alps icefield. *Quaternary Science Reviews*, *46*, 30-45

Haresign, E., and Warren, C. R. 2005. Melt rates at calving termini: a study at Glaciar León, Chilean Patagonia. *Geological Society, London, Special Publications*, *242*(1), 99-109

Hochstein, M. P., Watson, M. I., Malengreau, B., Nobes, D. C., and Owens, I. 1998. Rapid melting of the terminal section of the Hooker Glacier (Mt Cook National Park, New Zealand). *New Zealand Journal of Geology and Geophysics*, *41*(3), 203-218

Irwin, J. 1970. Lake Pukaki Provisional Bathymetry 1:31 680 New Zealand Oceanographic Institute Chart, Lake Series

James, W. H., Carrivick, J. L., Quincey, D. J., and Glasser, N. F. 2019. A geomorphology based reconstruction of ice volume distribution at the Last Glacial Maximum across the Southern Alps of New Zealand. *Quaternary Science Reviews*, *219*, 20-35

Kennett, M., Rolstad, C., Elvehoy, H., and Ruud, E. 1997. Calculation of drainage divides beneath the Svartisen ice-cap using GIS hydrologic tools. *Norsk Geografisk Tidsskrift-Norwegian Journal of Geography*, *51*(1), 23-28

Kirkbride, M. P. 1995. Relationships between temperature and ablation on the Tasman Glacier, Mount Cook National Park, New Zealand. *New Zealand Journal of Geology and Geophysics*, *38*(1), 17-27

Kleffmann, S., Davey, F., Melhuish, A., Okaya, D., Stern, T. 1998. Crustal structure in the central South Island, New Zealand, from the Lake Pukaki seismic experiment. New Zealand Journal of Geology and Geophysics 41, 39-49

Levy, R. H., Dunbar, G., Vandergoes, M., Howarth, J. D., Kingan, T., Pyne, A. R., Brotherston, G., Clarke, M., Dagg, B., Hill, M., and Kenton, E. (2018). A high-resolution climate record spanning the past 17 000 years recovered from Lake Ohau, South Island, New Zealand. *Scientific Drilling*

Long, D.T., Cox, S.C., Bannister, S., Gerstenberger, M.C., Okaya, D. 2003. Upper crustal structure beneath the eastern Southern Alps and the Mackenzie Basin, New Zealand, derived from seismic reflection data. New Zealand Journal of Geology and Geophysics 46, 21-40

Mallalieu, J., Carrivick, J. L., Quincey, D. J., & Smith, M. W. 2020. Calving seasonality associated with melt-undercutting and lake ice cover. *Geophysical Research Letters*

Marra, M. J., Shulmeister, J., and Smith, E. G. C. 2006. Reconstructing temperature during the Last Glacial Maximum from Lyndon Stream, South Island, New Zealand using beetle fossils and maximum likelihood envelopes. *Quaternary Science Reviews*, *25*(15-16), 1841-1849

McKinnon, K. A., Mackintosh, A. N., Anderson, B. M., and Barrell, D. J. 2012. The influence of sub-glacial bed evolution on ice extent: a model-based evaluation of the Last Glacial Maximum Pukaki glacier, New Zealand. *Quaternary Science Reviews*, *57*, 46-57

Mortensen, J., Lennert, K., Bendtsen, J., and Rysgaard, S. 2011. Heat sources for glacial melt in a sub-Arctic fjord (Godthåbsfjord) in contact with the Greenland Ice Sheet. *Journal of Geophysical Research: Oceans*, *116*

Motyka, R. J., O'Neel, S., Connor, C. L., and Echelmeyer, K. A. 2003. Twentieth century thinning of Mendenhall Glacier, Alaska, and its relationship to climate, lake calving, and glacier run-off. *Global and Planetary Change*, *35*(1-2), 93-112

Porter, S. C. 1975. Equilibrium-line altitudes of late Quaternary glaciers in the Southern Alps, New Zealand. *Quaternary research*, *5*(1), 27-47Purdie, H., Bealing, P., Tidey, E., Gomez, C., and Harrison, J. 2016. Bathymetric evolution of Tasman Glacier terminal lake, New Zealand, as determined by remote surveying techniques. *Global and Planetary Change*, *147*, 1-11

Roehl, K. 2002. Thermal regime of an ice-contact lake and its implication for glacier retreat. In *Ice in the Environment: Proceedings of the 16th IAHR International Symposium on Ice, Dunedin, New Zealand* (pp. 2-6)

Röhl, K. 2006. Thermo-erosional notch development at fresh-water-calving Tasman Glacier, New Zealand. *Journal of Glaciology*, *52*(177), 203-213

Sakai, A., Nakawo, M., and Fujita, K. 1998. Melt rate of ice cliffs on the Lirung Glacier, Nepal Himalayas, 1996. *Bull. Glacier Res*, *16*, 57-66

Sakakibara, D., and Sugiyama, S. 2014. Ice-front variations and speed changes of calving glaciers in the Southern Patagonia Icefield from 1984 to 2011. *Journal of Geophysical Research: earth surface*, *119*(11), 2541-2554

Samson, C. R., Sikes, E. L., and Howard, W. R. 2005. Deglacial paleoceanographic history of the Bay of Plenty, New Zealand. *Paleoceanography*, *20*(4)

Sikes, E. L., Howard, W. R., Neil, H. L., and Volkman, J. K. 2002. Glacial-interglacial sea surface temperature changes across the subtropical front east of New Zealand based on alkenone unsaturation ratios and foraminiferal assemblages. *Paleoceanography*, *17*(2), 2-1

Straneo, F., Hamilton, G. S., Sutherland, D. A., Stearns, L. A., Davidson, F., Hammill, M. O., and Rosing-Asvid, A. 2010. Rapid circulation of warm subtropical waters in a major glacial fjord in East Greenland. *Nature Geoscience*, *3*(3), 182-186

Stuefer, M., Rott, H., and Skvarca, P. 2007. Glaciar Perito Moreno, Patagonia: climate sensitivities and glacier characteristics preceding the 2003/04 and 2005/06 damming events. *Journal of Glaciology*, *53*(180), 3-16

Sutherland, J. L., Carrivick, J. L., Shulmeister, J., Quincey, D. J., and James, W. H. 2019. Ice-contact proglacial lakes associated with the Last Glacial Maximum across the Southern Alps, New Zealand. *Quaternary Science Reviews*, *213*, 67-92

Truffer, M., and Motyka, R. J. 2016. Where glaciers meet water: Subaqueous melt and its relevance to glaciers in various settings. *Reviews of Geophysics*, *54*(1), 220-239

Van der Veen, C. J. 2002. Calving glaciers. *Progress in Physical Geography*, *26*(1), 96-122

Venteris, E. R. 1999. Rapid tidewater glacier retreat: a comparison between Columbia Glacier, Alaska and Patagonian calving glaciers. *Global and Planetary Change*, *22*(1-4), 131-138

Warren, C. R., and Kirkbride, M. P. 2003. Calving speed and climatic sensitivity of New Zealand lake-calving glaciers. *Annals of Glaciology*, *36*, 173-178

Warren, C. R., Greene, D. R., and Glasser, N. F. 1995. Glaciar Upsala, Patagonia: rapid calving retreat in fresh water. *Annals of Glaciology*, *21*, 311-316

Warren, C., and Aniya, M. 1999. The calving glaciers of southern South America. *Global and Planetary Change*, *22*(1-4), 59-77